http://dx.doi.org/10.21611/qirt.1992.058

Lockin thermography for multiplex photothermal nondestructive evaluation

by D. WU, W. KARPEN and G. BUSSE

Institut für Kunststoffprüfung und Kunststoffkunde, Universität Stuttgart, Pfaffenwaldring 32,W-7000 Stuttgart 80, Germany

Abstract

The point by point thermal wave scan method is improved by combining it with the thermographic technique. The resulting lockin thermography can provide three images in a short time: phase image, magnitude image and thermographic image. Compared to thermography this technique has the advantage that phase angle images obtained in this way are not affected by non-uniformity of area heating and optical or infrared surface structure of the sample under investigation. An additional advantage is that due to parallel excitation of thermal waves one can use low modulation frequencies to obtain a larger depth range.

1. Introduction

Thermography is understood as an established technique where the defect induced perturbation of heat flow is monitored via the temperature field and related infrared emission. Thermography provides an image according to the Stefan-Boltzmann law. Advantages of thermography are its fast raster scan capability and also its commercial availability. However, there is no clear depth range defined since it depends also on defect size, extended structures may be detected at a larger distance. In the thermographic image thermal and optical infrared structures are superposed. One cannot distinguish clearly a thermal structure from the optical surface structure.

In transient thermography where heat is generated by a short light pulse one obtains depth information from time analysis of temperature.

Photothermal radiometry is one of the thermal wave detection techniques. By the measurement of modulated thermal infrared emission one can obtain phase and magnitude of local dynamic heat transport [1]. Thermal wave measurements performed in a raster-like fashion result in a thermal wave image. Depth range and resolution depend on modulation frequency and thermal diffusivity of material [2]. The phase is independent of optical/infrared surface structures and it is known to have a larger depth range than signal magnitude [3, 4].

The problem of photothermal radiometry imaging is that this is a point-by-point scan method which is slow especially at the low modulation frequencies required for a large depth range. The imaging time is proportional to the second power of depth. Therefore photothermal radiometry imaging has not yet found many industrial applications.

The infrared camera as a large scale thermal wave detector has been used by some authors [5, 6]. In this mode of operation the digital acquisition system is synchronised with the illumination system or with the modulated load generating a modulated temperature field around a fatigue crack [7].

http://dx.doi.org/10.21611/qirt.1992.058

2. Principle of lockin thermography

The purpose of this paper is to present a method which combines the advantages both of rapid scanning (which is used in conventional thermography) and modulated thermal waves.

The thermal wave is excited by optical absorption simultaneously on the whole sample surface. Each pixel on the sample surface is monitored sequentially using thermographic techniques and lockin data analysis. The signal analysis of a hardware lockin is simulated by a complex Fourier analysis of the digitized data points. If both the reference signal and thermal wave signal are sine-waves, four data points per modulation cycle are sufficient to provide the correct phase-angle and magnitude. This number of data points is the result of a trade-off between accuracy and time. More points will improve the signal to noise ratio while three points may require more time for evaluation whereas four data points have the advantage of a simplified evaluation. The principle of lockin thermography is shown in *figure 1*. During each modulation cycle four successive mirror-scans are performed to interrogate all pixels of the whole scan line. Therefore such mirror scans provide for each pixel (e.g. x_1) four signal data points S_1 to S_4 on its specific sinusoidal thermal wave. With these four obtained values one can calculate magnitude $A(x_1)$ and the phase shift $\varphi(x_1)$. An additional phase angle due to the time lag between subsequent pixels is easily corrected.

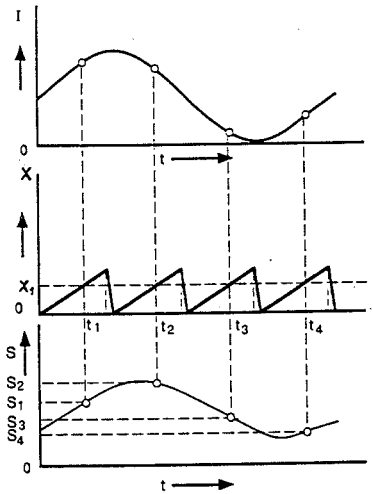

Fig. 1 - Principle of lockin thermography:
Time dependence of light intensity is shown together with scanning point x_1 from which the thermal wave curve S is constructed for x_1

$$A(x_1) = \sqrt{[S_3(x_1) - S_1(x_1)]^2 + [S_4(x_1) - S_2(x_1)]^2}$$

$$\varphi(x_1) = arctg \frac{S_3(x_1) - S_1(x_1)}{S_4(x_1) - S_2(x_1)}$$

$$T(x_1) = \frac{S_1(x_1) + S_2(x_1) + S_3(x_1) + S_4(x_1)}{4}$$

http://dx.doi.org/10.21611/qirt.1992.058

The average value of S_1 to S_4 is the local thermographic signal that one would find for a constant average temperature. Thermal wave magnitude A is affected by local optical absorption and infrared emission coefficients, local thermal properties and local optical illumination. However, in the equation for signal phase φ the effects of inhomogeneous illumination and of surface absorption/emission structure are eliminated because they are proportionalities that are cancelled in the ratio. Therefore a phase angle image reveals only thermal structures in the sample [8, 9].

3. Apparatus

Figure 2 shows the experimental setup of our lockin thermography. The whole sample surface was exposed to a sinusoidal illumination of a heating beam at a modulation frequency of 0.9 Hz [10]. A conventional halogen lamp (24 V/250 W) was controlled by the computer to generate a sinusoidal illumination power. The infrared filter was used to block off the infrared emission from the lamp which would confuse the infrared detector. During each modulation period four successive scans were performed to monitor all the surface pixel one after the other by a spatially resolved scanning radiometer.

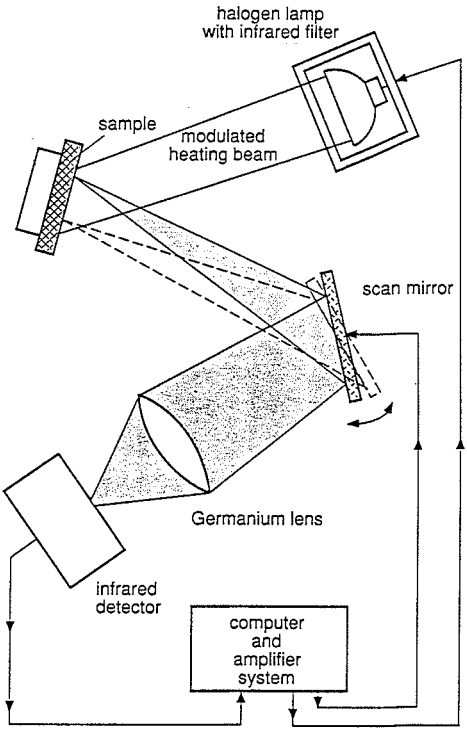

Fig. 2 - Block diagram of experimental arrangement used for obtaining thermal wave images with lockin thermography

http://dx.doi.org/10.21611/qirt.1992.058

4. Results

Figure 3 shows the result of a test performed in order to demonstrate that signal phase does not depend on the applied optical power density. The sample was painted metal where a stripe on the surface had been painted twice. Two line scans were performed, the second one at a reduced light intensity. Though all obtained curves reveal the region of increased paint thickness, the results from the two successive scans differ from each other for the thermographic signal and magnitude (*figure 3*). However, the two phase curves (each accumulated over 10 scans to improve the signal to noise ratio) are the same. A potentially relevant application example of lockin thermography is inspection of paint to reveal inhomogeneity of thickness.

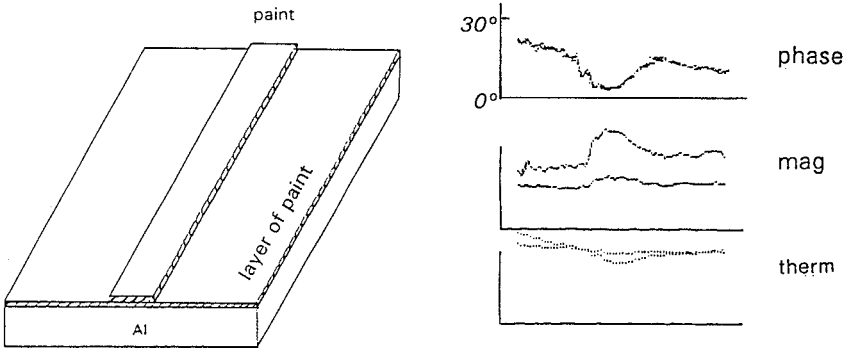

Fig. 3 - Sample geometry and results of line scans with phase, magnitude and thermography at two levels of illumination

Under this aspect a wedge shaped coating was painted on an iron substrate. The coating thickness ranged from about 50 µm to 100 µm. Modulation frequency was about 0.6 Hz. Phase and magnitude images both show this wedge shaped coating but magnitude image was disturbed by the non-uniformity of the surface heating (*figure 4*). The difference of thermography and phase is clearly seen when the sample is rotated by 180 degrees: the phase structure rotates as well while thermographic structure due to inhomogeneous illumination of course does not.

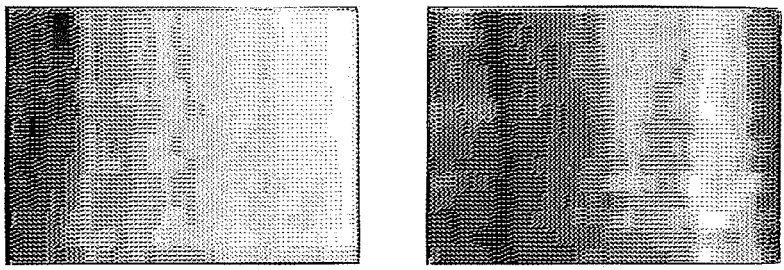

Fig. 4 - Lockin thermography images of the wedge shaped paint on an iron substrate with phase (a) and magnitude (b)

http://dx.doi.org/10.21611/qirt.1992.058

In another test we investigated a sample of carbon fiber reinforced polymer (CFRP) *(figure 5)*. A slot was milled into the rear surface of the sample to simulate thermal structure. The distance between surface and slot is constant. A white line was painted on the front surface to simulate optical and infrared surface structure. The result is that the thermography image shows mainly the white line. The magnitude image displays both thermal and optical structure while the phase image contains only the thermal structure. Similar results can be obtained with pulsed thermography where time of maximum temperature is related to defect depth and where optical structure can be eliminated by normalisation.

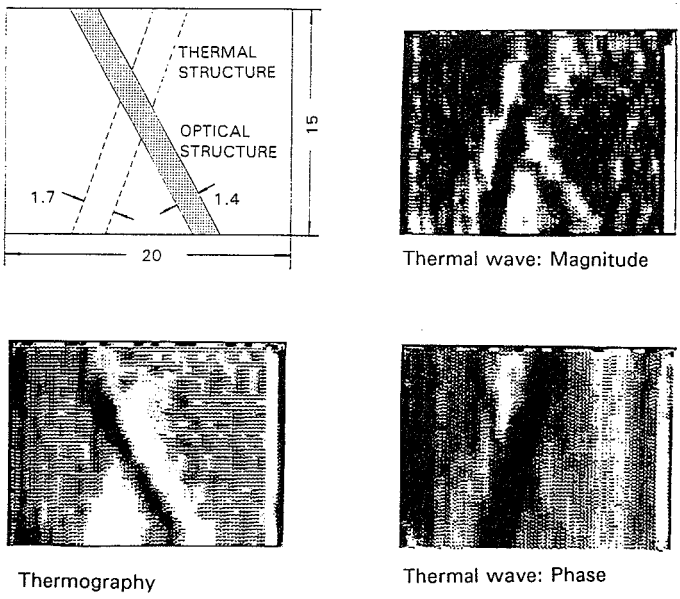

Fig. 5 - Lockin thermography of CFRP sample with thermal and optical/infrared surface structures

5. Conclusion

Lockin thermography bridges the gap between thermography and thermal waves. Compared to thermography the advantage is the capability of depth profiling and the suppression of optical surface structure to reveal only thermal structures. Compared to conventional thermal wave methods the imaging time is much shorter because the stationary thermal wave field is excited everywhere simultaneously and monitored sequentially in a multiplex mode.

However, lockin thermography still needs to be compared with pulsed thermography which is a competing technique. It is worthwhile to investigate under which conditions (sample, time, maximum optical power or energy) each technique should be favoured. This will be one task in our future work.

http://dx.doi.org/10.21611/qirt.1992.058

REFERENCES

[1] NORDAL (P.E.) and KANSTAD (S.O.) - *Photothermal radiometry.* Phys. Scripta 20, 1979, p. 659.

[2] ROSENCWAIG (A.) and GERSHO (A.) - *Theory of the photoacoustic effect with solids.* J. Appl. Phys. 47, 1976, p. 64.

[3] BUSSE (G.) - *Optoacoustic phase angle measurement for probing a metal.* Appl. Phys. Lett. 35, 1979, p. 759.

[4] THOMAS (R.L.), POUCH (J.J.), WONG (Y.H.), FAVRO (L.D.), KUO (P.K.) and ROSENCWAIG (A.) - *Subsurface flaw detection in metals by photoacoustic microscopy.* J. Appl. Phys. 51, 1980, p. 1152.

[5] BEAUDOIN (J.L.), MERIENNE (E.), DANJOUX (R.) and EGEE (M.) - *Numerical system for infrared scanners and application to the subsurface control of materials by photothermal radiometry.* Infrared Technology and Applications. SPIE Vol. 590, 1985, p. 287.

[6] FAVRO (L.D.), AHMED (T.), JIN (H.J.), KUO (P.K.) and THOMAS (R.L.) - *Noise suppression in IR thermal-wave video images by real-time processing in synchronism with active stimulation of the target.* SPIE Vol. 1313 Thermosense XII, 1990, p. 302.

[7] BOUC (R.) and NAYROLES (B.) - *Méthodes et résultats en thermographie infrarouge des solides.* J. de Mécanique théorique et appliquée 4, 1985, p. 27.

[8] ROSENCWAIG (A) and BUSSE (G.) - *High resolution photoacoustic thermal wave microscopy.* Appl. Phys. Lett. 36, 1980, p. 725.

[9] BUSSE (G.) - *Optoacoustic and photothermal material inspection techniques.* Appl. Opt. 21, 1982, p. 107.

[10] BUSSE (G.), WU (D.) and KARPEN (W.) - *Thermal wave imaging with phase sensitive modulated thermography.* J. Appl. Phys. 71 8, 1992, p. 3962.